[3]. Both therapies have been proven to be effective for visceral, hematologic and skeletal abnormalities [4–6]. Unfortunately, the efficacy of these therapies to neurological manifestations is, if any, limited [7–10].

It has been known that some of the disease-causing mutations of β-Glu do not interfere with its catalytic activity but disrupt either its proper folding in the endoplasmic reticulum (ER) or intracellular trafficking out of this compartment. Recent evidence suggested that the mutant proteins, retained in the ER because of improper folding or trafficking, were degraded by the proteasome in a series of processes summarized as ERAD (ER-associated protein degradation) [11,12]. This bases the idea of "enzyme enhancement therapy", a novel therapeutic strategy for GD, which aims at stabilization and rescue of the mutant enzyme by using cell-permeable small molecules [13,14]. In pursuit of this idea, we have shown that a carbohydrate mimic *N*-octyl-β-valienamine (NOV), an inhibitor of β-Glu, could increase the protein level and enzyme activity of F213I mutant β-Glu in cultured GD fibroblasts [15], whereas Sawkar and colleagues reported that *N*-nonyl-deoxynojirimaycin (NN-DNJ), another inhibitor of β-Glu, could increase the enzyme activity of N370S and G202R mutants [16,17]. In a recent review by Bernier et al. [18], the term "chemical chaperone" was used to describe molecules that help folding of proteins in a nonspecific manner, whereas those with specific effects on the target protein were termed "pharmacological chaperone". In addition, the term "enzyme enhancement activity (EEA)" is defined as an activity of a molecule to increase the cellular enzyme activity when the molecule is applied to live cells [14].

The purpose of the current study was to further explore the potential of NOV as a pharmacological chaperone for β-Glu mutant proteins. For this purpose, we examined EEA of NOV in cultured human GD fibroblasts as well as in COS cells transiently expressing recombinant mutant proteins. Since we found that NOV was effective on both N370S and G202R mutants, we compared EEA of NOV and that of NN-DNJ. We also tested activities of *N*-alkyl-β-valienamines with various lengths of the acyl chain on the F213I mutant.

2. Materials and methods

2.1 Materials

Dulbecco's Modified Eagle's Medium (DMEM), bovine calf serum (BCS) and LipofactAMINE reagent were obtained from Life Technologies Inc. *N*-alkyl-β-valienamine hydrochlorides were synthesized in our laboratory (Central Research Laboratories, Seikagaku Co.). Stock solution of the compounds was prepared in H_2O at 3 mM and stored at −20 °C. Anti-Flag M2 affinity gel and rabbit polyclonal anti-Flag antibody were from Sigma. Endoglycosidase-H was from New England Biolabs.

2.2. Construction of β-Glu expression plasmids

Human β-Glu cDNA (a kind gift from Dr. S. Tsuji, Tokyo University) was subcloned into a mammalian expression vector pCAGGS. A Flag-epitope was introduced to the C-terminus of the cDNA by PCR. The following mutations were introduced by using the Quick Change site-directed mutagenesis kit: N188S, G193W, G202R, F213I, N370S and L444P. All the mutations were confirmed by direct sequencing.

2.3. Cell culture

Human skin fibroblasts and COS cells were cultured in DMEM/10% BCS at 37 °C in 5% CO_2. We used one control cell line (H8) and 9 lines of GD cells. 6 lines of GD cells were from Japanese patients. 4 cell lines carried β-Glu mutations of F213I/F213I, G202R/L444P, N188S/G193W and nt1447del20insTG/L444P, whereas in the other 2 cell lines, only one β-Glu mutation, nt1447del20insTG or D409H, was identified and the mutation on the other allele was left unknown [19]. The other 3 lines of GD cells that carried the N370S mutation were from Caucasian patients: two cell lines (DMN00.41 and DMN87.30) carried N370S homozygous mutations and one cell line carried N370S/84GG. Both 84GG and nt1447del20insTG are predicted to cause premature termination of the encoded protein. Culture medium was replaced every 2 days with fresh media supplemented with or without *N*-alkyl-β-valienamines at the indicated concentrations. COS cells in 35-mm dishes were transfected with β-Glu cDNA by using LipofactAMINE according to manufacturer's instructions. 24 h post-transfection, cells were treated with or without the compounds for 24 h.

2.4. Immunoprecipitation and immunoblotting

All procedures were carried out at 4 °C. COS cells were lysed by sonication in PBS supplemented with 1% Triton X-100 and a protease inhibitor cocktail (Boehringer). After a brief centrifugation to remove insoluble material, the supernatant was precleared with an aliquot of agarose beads. For immunoprecipitation of Flag-β-Glu, the lysates (500 μl from a 35-mm dish) were incubated for 16 h with anti-Flag M2 agarose beads (20 μl of 50% slurry). The beads were washed with PBS/1% Triton X-100, rinsed with H_2O and the final volume of the precipitates was adjusted to 40 μl with H_2O. For the enzyme assay, 4 μl of the precipitates was used as described below. For immunoblotting, bound proteins were eluted by incubation of 20 μl of precipitates with the same volume of 2× SDS-PAGE sample buffer at 100 °C for 3 min. SDS-PAGE and Western transfer were carried out as previously described [15]. The blots were probed with rabbit polyclonal anti-Flag antibody and developed using an ECL kit (Amersham Pharmacia).

2.5. In vitro enzyme assay

β-Glu activities in cell lysates or immunoprecipitates were determined by using 4-methylumbelliferone-conjugated β-D-glucopyranoside as a substrate [20]. For preparation of cell lysates, cells in 35-mm dishes were scraped into 100 μl of ice-cold H_2O and lysed by sonication. Insoluble materials were removed by centrifugation and protein concentrations were determined with a BCA microprotein assay kit. Anti-Flag immunoprecipitates were prepared as described above. 4 μl of the lysates or immunoprecipitates was incubated at 37 °C with 8 μl of the substrate solution in 0.1 M citrate buffer, pH 5.2, supplemented with sodium taurocholate (0.8% w/v). The reaction was terminated by adding 0.4 ml of 0.2 M glycine sodium hydroxide buffer (pH 10.7). Liberated 4-methylumbelliferone was measured with Perkin Elmer Luminescence Spectrometer (excitation wave length: 340 nm; emission: 460 nm). One unit of enzyme activity was defined as nmol of 4-methylumbelliferone released per hour and normalized for the amount of protein contained in the lysates.

2.6. Intact cell enzyme assay

β-Glu activities in live cells were estimated by the methods described by Sawkar et al. [16]. Briefly, cells in 24-well plates were treated with NOV or NN-DNJ for 4 days. After washing with PBS, the cells were incubated in 80 μl of PBS and 80 μl of 0.2 M acetate buffer (pH 4.0). The reaction was started by addition of 100 μl of 4-methylumbelliferyl-β-D-glucoside (5 mM), followed by incubation at 37 °C for 1 h. The reaction was stopped by lysing the cells by the addition of 2 ml of 0.2 M glycine buffer (pH 10.7) and liberated 4-methylumbelliferone was quantified. Every experiment was performed in

parallel with cells that had been preincubated with or without conduritol B epoxide (CBE: Toronto Research Chemicals) at 0.5 mM for 1 h. The CBE-sensitive component was ascribed to lysosomal β-Glu, whereas the CBE-insensitive component was ascribed to non-lysosomal β-Glu.

2.7. Endoglycosidase-H treatment

Cell lysates (in H_2O containing ~40 μg protein) from transfected COS cells were incubated at 100 °C for 10 min with 0.5% SDS and 40 mM DTT to denature proteins. They were then incubated at 37 °C for 1 h with 0.5 unit of endoglycosidase-H (Endo-H) in 50 mM citrate buffer (pH 5.5). The reaction mixture was subjected to SDS-PAGE, Western transfer and anti-Flag immunoblotting as described above.

2.8. Immunofluorescence

We used staining procedures described previously [15]. Briefly, COS cells grown on cover glasses were transfected with Flag-β-Glu cDNA and 24 h post-transfection, exposed to Lysotracker Red (0.5 μM; Molecular Probe) for 1 h. Cells were fixed with 4% paraformaldehyde and permeabilized with 1% TritonX-100. They were incubated with rabbit polyclonal anti-Flag antibody (1:500), followed by Alexa488-conjugated anti-rabbit IgG. Fluorescent images were collected by using a Leica TSC SP2 confocal laser microscope.

3. Results

3.1. EEA of NOV in human GD fibroblasts assessed by ex vivo enzyme assay

In our previous study [15], EEA of NOV was evaluated by ex vivo experiments in which GD cells were treated with NOV for 4 days followed by determination of the enzyme activity in cell lysates. By this method, we found significant EEA of NOV in F213I homozygous and heterozygous (F213I/L444P) cells. The maximum response was obtained at an NOV concentration of 30 μM in F213I homozygous cells. NOV was ineffective in cells with mutations of N370S/84GG, L444P/L444P and L444P/RecNcil.

N-alkyl-β-valienamine preparations, including NOV, used in our previous study were poorly soluble in water, and hence in culture medium. Although NOV had the best solubility among the *N*-alkyl-β-valienamines, it was barely soluble in water above 3 mM. To test whether the water-solubility affected EEA, we prepared hydrochloride forms of *N*-alkyl-β-valienamines (see Fig. 4a), which were easily soluble in water above 30 mM. By using the hydrochloride form of NOV, we could reproduce EEA of NOV in F213I homozygous cells but with a different dose–response profile: the maximum response was obtained at 3 μM (Fig. 1a). Because of this improved efficacy, hydrochloride preparations were used in all the subsequent experiments.

In the 7 lines of GD cells newly included in the screening, we found statistically significant EEA of NOV in four lines of cells with mutations of N188S/G193W, G202R/L444P and N370S/N370S. NOV effects on the two cell lines with N370 homozygous mutations were remarkably similar to each other, causing an ~2-fold increase at concentration of 3 and 30 μM. In accordance with the results in our previous study [15], NOV elicited weak EEA in N370S/84GG cells, although the increase was not statistically significant. In contrast, NOV elicited no effects in cells with mutations of nt1447del20insTG/L444P. In two cell lines, only one mutation of β-Glu, D409H or nt1447del20insTG, was identified, and the mutation on the other allele was left unknown. NOV effects were also negative in these two lines of cells (Fig. 1a).

3.2. EEA of NOV and NN-DNJ assessed by intact cell enzyme assay

The above ex vivo enzyme assay did not indicate whether the lysosomal enzyme activity was enhanced by NOV. To compensate for this, we employed "intact cell enzyme assay" described by Sawkar et al. [16], in which the cellular enzyme activity was estimated by application of the substrate (4-methylumbelliferone-conjugated β-D-glucopyranoside) to intact cells followed by quantification of liberated 4-methylumbelliferone. In this assay, cells were pretreated with or without a high concentration (0.5 mM) of conduritol B epoxide (CBE), an irreversible inhibitor of lysosomal β-Glu, before exposure to the substrate. In wild-type cells, more than 95% of the total cellular enzyme activity was sensitive to CBE, suggesting that the degradation was mostly due to lysosomal enzyme activity. There were no significant differences in the absolute values of the CBE-insensitive activity (i.e., non-lysosomal enzyme activity) between control and GD cells (data not shown).

In accordance with the results of ex vivo enzyme assay, NOV was effective in cells with mutations of F213I/F213I, N188S/G193W, G202R/L444P and N370S/N370S, but not in cells with mutations of L444P/RecNcil, L444P/L444P and D409H/unknown (Fig. 1b). In contrast to the results of ex vivo enzyme assay, however, NOV was clearly effective on N370S/84GG cells. We also evaluated EEA of NN-DNJ and found significant effects of this compound in cells with mutations of N370S/N370S and N370S/84GG. This result was in accordance with the report by Sawkar et al. [17] who found EEA of NN-DNJ in cells with homozygous mutations of N370S and G202R. NN-DNJ was also effective in cells with mutations of F213I/F213I. Although the increases were not statistically significant, NN-DNJ elicited weak EEA in cells with mutations of N188S/G193W and G202R/L444P, whereas it was not at all effective in cells with mutations of L444P/RecNcil, L444P/L444P and D409H/unknown. Thus, it appeared that the two compounds, NOV and NN-DNJ, shared the same selectivity on β-Glu mutations. In addition, neither NOV nor NN-DNJ affected the levels of CBE-insensitive, non-lysosomal enzyme activity (data not shown).

Given the similar effects of NOV and NN-DNJ, we examined whether these two compounds acted synergistically or not. When F213I/F213I cells were exposed to NOV and NN-DNJ (both at 3 μM) simultaneously, the effects were not additive, but EEA of NOV was rather diminished (Fig. 1b). Similar findings were reproduced in N188S/G193W and G202R/L444P cells. In two lines of N370 homozygous cells and N370S/84GG cells, NN-DNJ did not reduce EEA of NOV, but again the effects of these two compounds were not additive. To further confirm this lack of co-operation, we evaluated in vitro inhibitory activity of NN-DNJ in the presence or absence of NOV and found that NOV caused a dose-dependent decrease in the efficacy of NN-DNJ (Fig. 1c). The IC_{50} values for NN-DNJ were 0.31±0.03

and 1.6±0.31 μM (means±SEM, $n=3$), in the absence and presence of NOV (3 μM), respectively. This NOV effect was not specific for NN-DNJ but a similar decrease in the inhibitory activity was also observed for CBE. As a negative control, *N*-butyl-β-valienamine, which has a very weak in vitro inhibitory activity (see Fig. 4), failed to affect the activities of NN-DNJ and CBE.

3.3. EEA of NOV on recombinant mutant β-Glu expressed in COS cells

Primary-cultured human cells have several disadvantages for evaluation of EEA, including their genetic heterogeneity and heterozygosity of the mutations. For example, we could not tell from the positive effect of NOV in N188S/G193W cells which

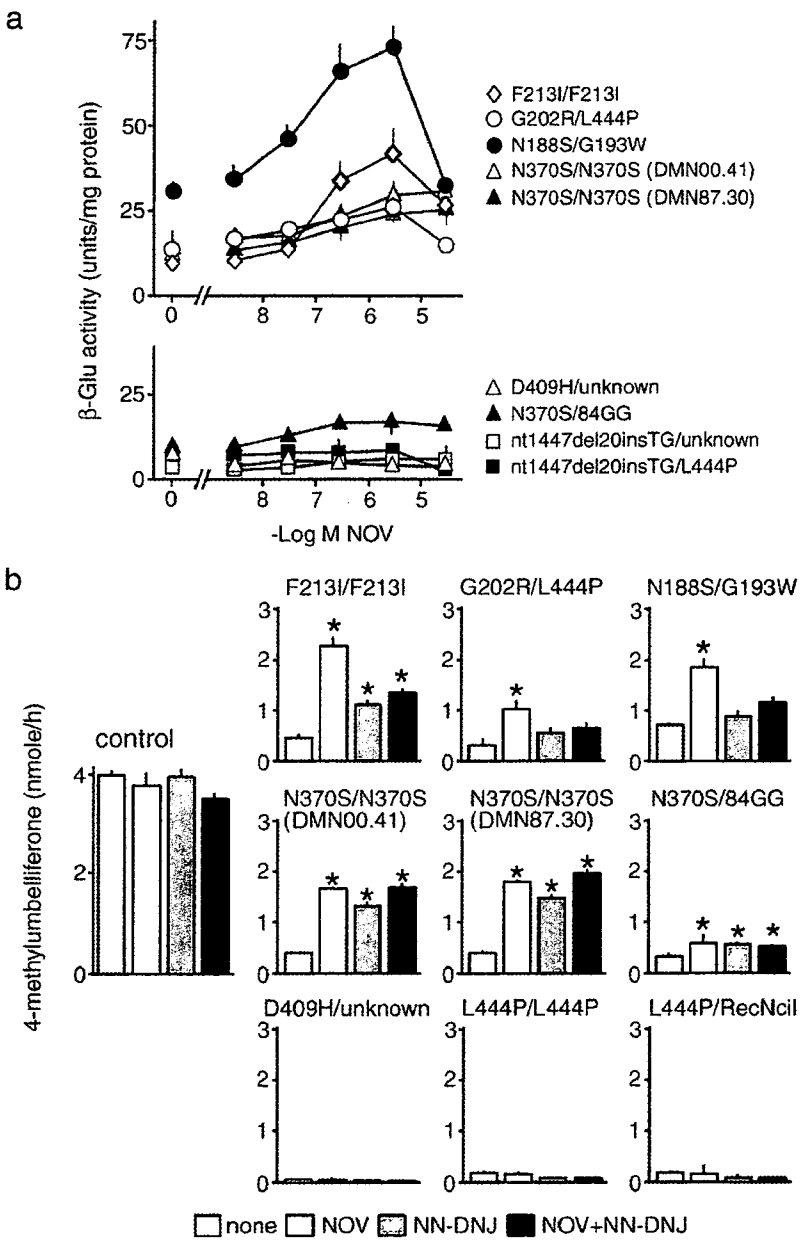

Fig. 1. EEA of NOV and NN-DNJ on mutant β-Glu in GD fibroblasts. (a) Ex vivo enzyme assay. 9 lines of GD cells were cultured for 4 days in the absence or presence of increasing concentrations of NOV and β-Glu activity in cell lysates was determined. The data from cells with positive responses to NOV were shown in the upper panel whereas those with negative responses were shown in the lower panel. Each point represents the mean±SEM of 3 determinations each done in triplicate. Red marks indicate that the values are statistically different from the values in the absence of the drug ($*p<0.05$, *t* test). (b) Intact cell enzyme assay. GD cells were cultured for 4 days in the absence or presence of NOV and/or NN-DNJ (both at 3 μM). Lysosomal β-Glu activity was estimated in intact cells as described in Materials and methods. Each bar represents the mean±SEM of 3 determinations each done in triplicate. $*p<0.05$, statistically different from the values in the absence of the drug (*t* test). (c) Effects of NOV on in vitro inhibitory activities of NN-DNJ and CBE. Inhibitory activities of NN-DNJ and CBE against β-Glu in lysates from a control cells were determined in the absence or presence of NOV (upper panels). As a control, the same experiments were repeated with *N*-butyl-β-valienamine (lower panels). Each point represents the mean of duplicates obtained in a single experiment. Similar results were reproduced twice.

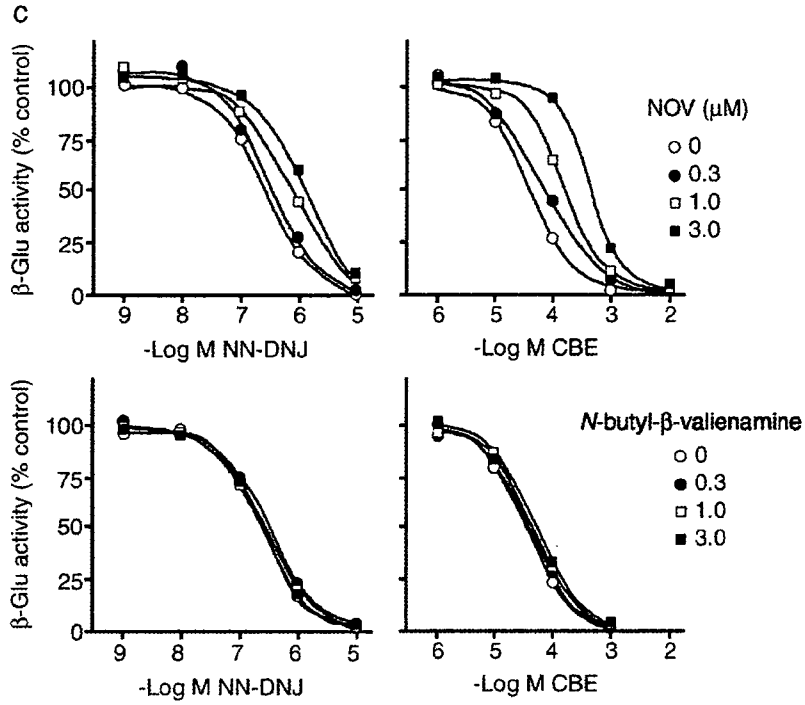

Fig. 1 (*continued*).

of the two mutants (or both of them) responded to NOV. As an alternative method to evaluate EEA, we used heterologous expression of recombinant β-Glu in COS cells. A problem with this system was the endogenous β-Glu activity of COS cells. To circumvent this problem, we placed a Flag-epitope at the C-terminus of recombinant β-Glu and determined the enzyme activity recovered in anti-Flag immunoprecipitates. Practically, 24 h after transfection, the cells were exposed to NOV for another 24 h, and cell lysates were subjected to anti-Flag M2 immunoprecipitation. As shown in Fig. 2a, the immunoprecipitates from mock-transfected cells contained virtually no activity whereas those from cells transfected with mutant Flag-β-Glu contained various levels of activities. The relative levels of the activities in immunoprecipitates (Fig. 2a, right panel) faithfully reflected the relative levels in lysates (left panel), suggesting similar efficacies of immunoprecipitation between the different constructs.

By using this immunoprecipitation/enzyme assay, we evaluated EEA of NOV on the wild-type and 6 kinds of β-Glu mutants and found dose-dependent, positive effects on N188S, G202R, F213I and N370S mutants, and negative effects on G193W and L444P mutants (Fig. 2b). The profiles of dose-dependence were different from those in human cells: with the exception of N188S, the maximum effects of NOV were obtained at 10 μM, the highest concentration applied. The effect on the wild-type β-Glu was negative. EEA of NOV on the 4 kinds of mutants were statistically significant as analyzed using the data at an NOV concentration of 10 μM (Fig. 2c). Anti-Flag Western blotting of immunoprecipitation products showed that NOV caused dose-dependent increases in the protein levels of N188S, G202R and F213I mutants. The protein levels of N370S mutant was marginally increased by NOV, whereas the levels of G193W and L444P mutants were not at all affected (Fig. 2b).

3.4. Intracellular localization and processing of recombinant β-Glu expressed in COS cells

In our previous study using F213I homozygous human cells [15], we could show by immunofluorescence and cell fractionation experiments that NOV restored lysosomal localization of the mutant β-Glu. Having shown EEA of NOV on the recombinant proteins expressed in COS cells, we examined whether there were any differences in the intracellular localization and processing of the proteins between the wild-type and mutants, and whether NOV caused any alterations.

Anti-Flag immunofluorescence of the wild-type Flag-β-Glu showed reticular distribution throughout the cytosol, indicating its predominant localization in the ER. The anti-Flag signals showed little co-localization with Lysotracker red (Fig. 3a, upper panels). This distribution was in contrast to lysosomal localization of the endogenous, wild-type β-Glu in human fibroblasts [15], but was not specific to COS cells. Similar intracellular distribution was reproduced in CHO, HeLa and HEK293 cells (data not shown). This distribution was neither specific for the Flag-tagged protein because similar distribution was observed for recombinant proteins tagged with a myc-epitope or GFP (data not shown).

Like the wild-type protein, F213I mutant Flag-β-Glu (Fig. 3a, middle panels) as well as other mutant proteins (data not shown) were mainly localized in the ER and did not co-localize with Lysotracker red. To confirm this localization, we

tested sensitivity of expressed proteins to Endo-H digestion (Fig. 3b). Anti-Flag Western blotting of the wild-type Flag-β-Glu gave two bands: the major band at 66 kDa and the minor band at 62 kDa, which represented the immature ER form and the mature post-Golgi form, respectively [11]. As expected, Endo-H digestion abolished the 66 kDa band and yielded a band at 58 kDa, which corresponds to the non-glycosylated protein, whereas it barely affected the 62 kDa band. The same

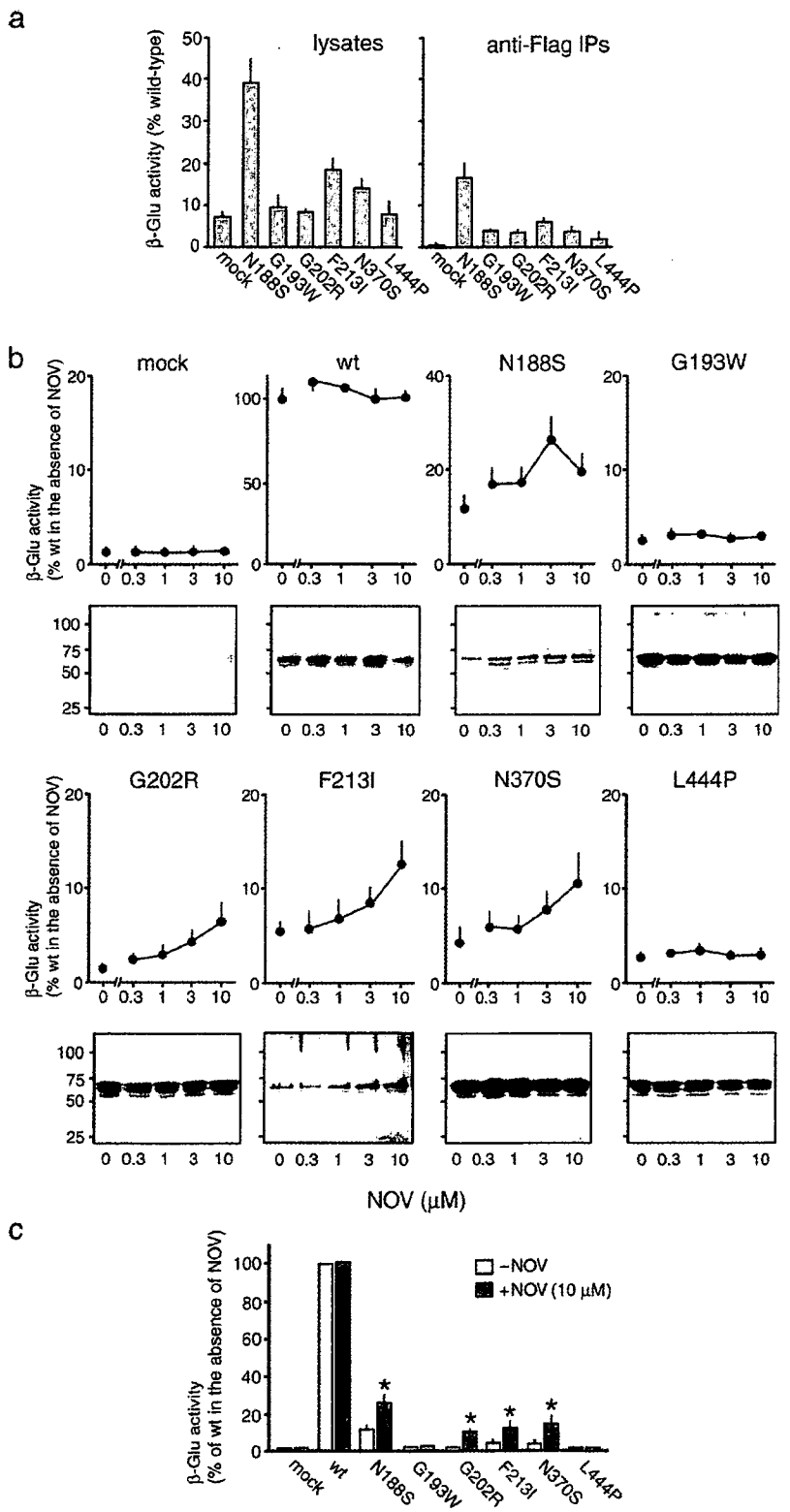

experiments on mutant proteins revealed similar results, confirming predominant localization in the ER of both wild-type and mutant proteins in COS cells.

NOV treatment of transfected cells failed to alter the intracellular distribution and processing of expressed proteins, as assessed by anti-Flag immunofluorescence (Fig. 3a, lower panels) and Endo-H digestion (Fig. 3b). These findings suggested that the site of action of NOV was the ER, consistent with our assumption that it acted as a pharmacological chaperone to protect mutant proteins from ERAD. However, these results also indicated that the heterologous expression was inappropriate as an experimental system to assess lysosomal transport of rescued proteins.

3.5. EEA of N-alkyl-valienamines related to NOV

All of the pharmacological chaperones for mutant lysosomal enzymes described so far are inhibitors of the target enzyme [21]. The hypothesis "the best chaperone is the best inhibitor" postulates that the activity of a molecule as a chaperone depends on its binding affinity to the target enzyme, and hence on its inhibitory activity [22]. We have shown previously that the in vitro inhibitory activity of *N*-alkyl-β-valienamines against β-Glu depended on the number and the length of the acyl chain [23,24]. To examine whether the above hypothesis holds true for *N*-alkyl-β-valienamines, we prepared compounds with various lengths of the acyl chain and compared their in vitro inhibitory activities and EEA. Compounds **a**–**e** listed in Fig. 4a contained a single acyl chain with various lengths, whereas compound **f** contained double acyl chains. Compound **g** carried a glucopyranosyl head group instead of a valienamine head group, and was included as a negative control.

In vitro inhibition experiments using cell lysates from control human fibroblasts revealed that compound **f** with double acyl chains was the best β-Glu inhibitor among these compounds, with the following rank order of potency: **f>b, e>c, d>a, g** (Fig. 4b, and the IC_{50} values were given in Fig. 4a). Immunoprecipitation/enzyme assays using COS cells transfected with F213I mutant Flag-β-Glu showed that compound **c** (*N*-dodecacyl-β-valienamine) exhibited EEA, which was as potent as that of compound **b** (NOV). Compound **d** exhibited week EEA, whereas compounds **e** and **f** rather suppressed the enzyme activity. Compounds **a** and **g**, both of which had a weak in vitro inhibitory activity, failed to alter the enzyme activity of the F213I mutant (Fig. 4c, and the relative efficacies were summarized in Fig. 4a). These findings indicated that the simple "the best chaperone is the best inhibitor" hypothesis did not hold true for *N*-alkyl-β-valienamines, and suggested that the presence of a single acyl chain with an appropriate length (i.e., carbon numbers between 8 and 14) was necessary for them to act as a chaperone for mutant β-Glu.

4. Discussion

In the current study, we evaluated EEA of NOV in human GD cells using two assays: ex vivo enzyme assay (Fig. 1a) and intact cell enzyme assay (Fig. 1b). With the exception of N370S/84GG cells, these two assays gave the same results: NOV exhibited EEA in 5 GD cell lines with mutations of F213I/F213I, N188S/G193W, G202R/L444P and N370S/N370S, whereas it was ineffective in cells with mutations of L444P/L444P, L444P/RecNciI and D409H/unknown. It was also ineffective in cells with mutations of nt1447del20insTG/L444P and nt1447del20insTG/unknown, in ex vivo enzyme assay. NOV was only marginally effective in N370S/84GG cells as assessed by ex vivo enzyme assay whereas it caused clear EEA in the same cells as assessed by intact cell enzyme assay. The precise reason for this discrepancy was left unknown, but it may suggest that intact cell enzyme assay was more sensitive than ex vivo enzyme assay to detect EEA.

Using heterologous expression of recombinant Flag-tagged β-Glu in COS cells, we could further confirm EEA of NOV (Fig. 2). It was effective on N188S, G202R, F213I and N370S mutants but was ineffective on G193W and L444P mutants. These results confirmed the selective effects of NOV on individual mutants as expected from its effects in human cells. Besides, this analysis suggested that EEA of NOV on N188S/G193W human cells reflected its selective effect on N188S mutant. Anti-Flag Western blotting showed that NOV-induced increase in the enzyme activity was accompanied by increased protein levels of the mutant proteins, consistent with an action of NOV as a pharmacological chaperone. The identical genetic background of this heterologous expression system is a clear advantage over human cells to assess EEA. However, it also had a disadvantage that, unlike the endogenous protein, the expressed protein was retained in the ER (Fig. 3) and hence the lysosomal transport of rescued protein could not be assessed. Nonetheless, the heterologous expression system will be a useful alternative to evaluate EEA when human cells with specific mutations are not available.

Studies on genotype–phenotype relationships in human patients have shown that except for the N370S mutation, which is exclusively associated with type I, non-neuronopathic form, the other three mutations with positive responses to NOV

Fig. 2. Effects of NOV on recombinant β-Glu expressed in COS cells. COS cells were transfected with Flag-tagged β-Glu constructs. 24 h post-transfection, cells were treated with or without NOV for 24 h. (a) Basal activities of β-Glu in cell lysates (left panel) and anti-Flag immunoprecipitation (IP) products (right panel). The activities were expressed as relative to that of the wild-type protein (100%). The values for the wild-type protein in lysates and IP products were 132±16 and 310±12 nmol/mg protein/h (means±SEM, $n=3$), respectively. (b, c) Effects of NOV on protein levels and activities of recombinant β-Glu in anti-Flag IP products. In b, cells were treated with or without increasing concentrations of NOV and the IP products were subjected to in vitro enzyme assay or anti-Flag immunoblotting as described in Materials and methods. Molecular weights are given on the left (kDa). The data with NOV concentrations at 0 and 10 μM were depicted in a bar graph in c for comparison of NOV effects on individual mutants. All in a–c, each bar or point represents mean±SEM of more than 3 determinations. $^*p<0.05$, statistically different from the values in the absence of the drug (*t* test).

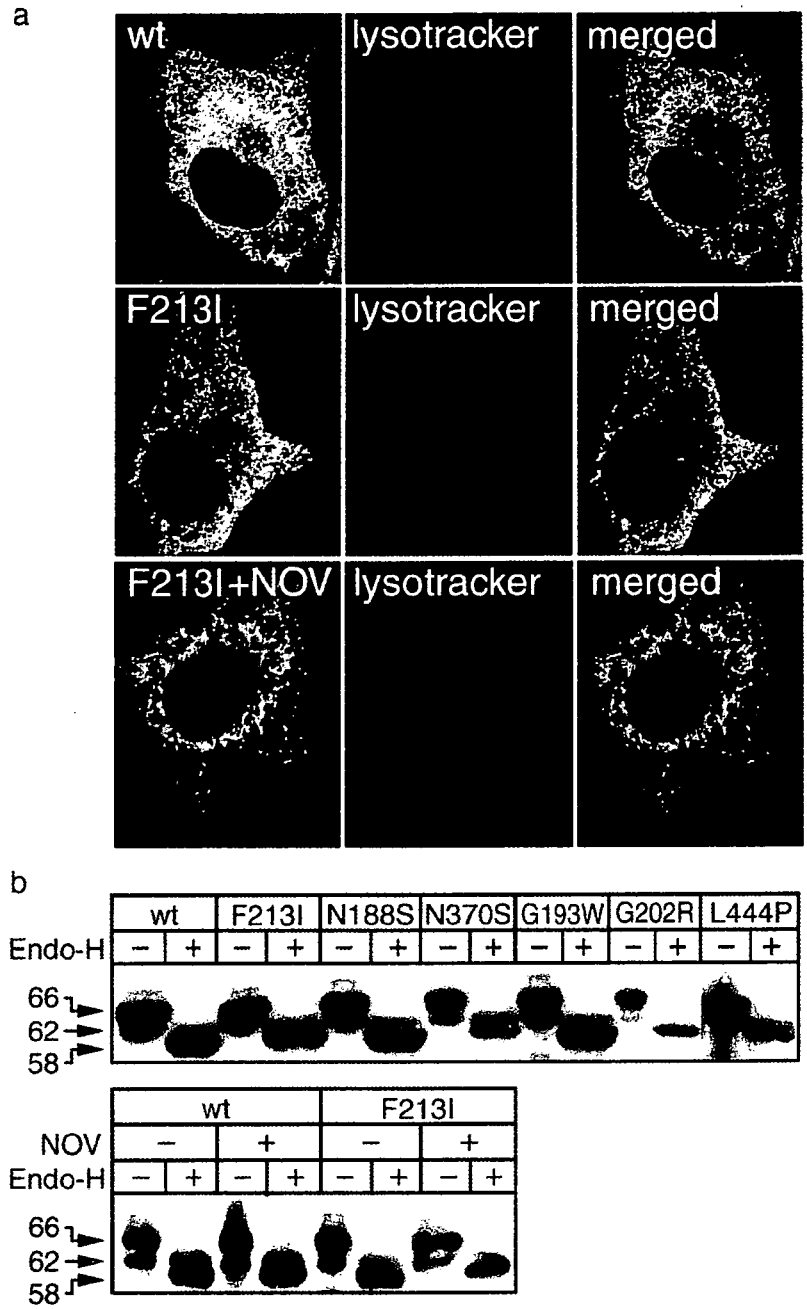

Fig. 3. Intracellular localization and processing of recombinant β-Glu expressed in COS cells. (a) Immunofluorescence. Cells were transfected with wild-type Flag-β-Glu (upper panels) or F213I mutant. Cells transfected with F213I mutant were cultured for 24 h in the absence (middle panels) or presence (lower panels) of NOV (10 μM). They were exposed to Lysotracker red before fixation and stained with anti-Flag antibody. Bound antibody was visualized with Alexa488-conjugated secondary antibody. Shown are the images obtained with a confocal microscope. (b) Endo-H sensitivity. Lysates from cells transfected with each Flag-β-Glu construct were subjected to Endo-H digestion followed by SDS-PAGE and anti-Flag immunoblotting (upper panel). Cells transfected with wild-type Flag-β-Glu or F213I mutant were treated with or without NOV (lower panel). Molecular weights are given on the left (kDa). All results shown were representative and were reproduced at least twice.

(N188S, G202R, F213I), can be associated with type 2 or 3, neuronopathic forms [19,25].

Recently, X-ray crystallography of human β-Glu revealed that it consisted of three structural domains [26]. Domain III contains the catalytic site, whereas the functional significance of domains I and II is left unknown. All the mutations with positive responses to NOV (N188S, G202R, F213I and N370S) were located in domain III, whereas those with negative responses, L444P and D409H were located in domain II and I, respectively. Since NOV is a structural mimic of the substrate, it is expected to bind to domain III. Therefore, localization of the mutations in domain III might be a prerequisite to pharmacological rescue of

a

	n	compound	IC_{50} (μM)	inhibition	EEA (F213I)
a	3	*N*-butyl-β-valienamine	>10	−	−
b	7	*N*-octyl-β-valienamine	0.502	+	++
c	11	*N*-dodecyl-β-valienamine	0.085	++	++
d	13	*N*-tetradecyl-β-valienamine	0.093	++	+
e	17	*N*-octadecyl-β-valienamine	0.442	+	−
f	7 (double)	*N*, *N*-octyl-β-valienamine	0.003	+++	−
g	7	octyl-β-glucopyranosylamine	>10	−	−

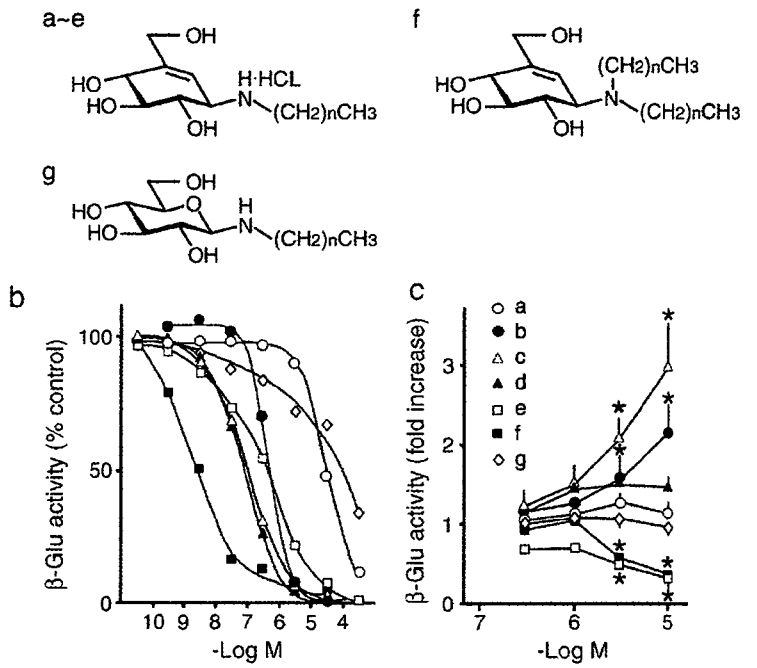

Fig. 4. Profiling of *N*-alkyl-β-valienamines. (a) Chemical structures of the compounds evaluated in this study. Compounds **a**–**f** are *N*-alkyl-β-valienamines with different acyl chains. They are all in a hydrochloride form, except for f. Compound g contains a glucopyranosyl head group instead of a valienamine head group. (b) In vitro inhibition of β-Glu. β-Glu activity in lysates from control human fibroblasts was determined in the absence or presence of increasing concentrations of each compound. Each point represents the mean of triplicate determinations obtained in a single experiment. IC_{50} values for individual compounds (means of three independent determinations) were given in a. (c) EEA on F213I mutant β-Glu expressed in COS cells. Cells transfected with F213I mutant Flag-β-Glu were incubated in the absence or presence of increasing concentrations of each compound. β-Glu activity of anti-Flag immunoprecipitates was determined as described in Materials and methods. Values were shown as relative to the values in the absence of any compound. Each point represents the mean±SEM of 3 determinations. $^*p<0.05$, statistically different from the values in the absence of any compound (*t* test).

the mutant proteins by NOV. However, an alternative possibility remains that the selective effects of NOV simply reflected the degree of instability of individual mutant proteins.

By using intact cell enzyme assay in human GD cells, we compared effects of NOV and NN-DNJ and found similar responses of individual cells to the two compounds (Fig. 1b). This was not surprising, given that NN-DNJ was also a structural mimic of the substrate and was expected to act in a manner similar to NOV. An important finding was that these two compounds did not work synergistically, but simultaneous addition of the two rather suppressed the action of each compound. Although the molecular mechanism for this lack of co-operation was left unknown, suppression of in vitro inhibitory activity of NN-DNJ by NOV (Fig. 1c) suggested that the presence of NOV hindered the binding of NN-DNJ to the enzyme, and vice versa.

We have shown that the optimal concentration of the hydrochloride form of NOV to elicit EEA on F213I homozygous cells was 10 times lower than that of the non-hydrochloride form, most likely because of its better solubility in the medium (Fig. 1a). By profiling the activities of *N*-alkyl-β-valienamines, we also found that *N*-dodecacyl-β-valienamine elicited EEA as potent as that of NOV (Fig. 4). In addition, NOV appeared to work better than NN-DNJ at the same concentration, at least in intact cell enzyme assay using human cells (Fig. 1b). These findings in cultured cells, however, do not allow us to predict which compound works best as a pharmacological chaperone in whole animals, and hence has the best therapeutic value. To prove the activity of *N*-octyl-β-epi-valienamine, an isomer of NOV, as a pharmacological chaperone for mutant β-galactosidase, we developed transgenic mice that lacked the endogenous wild-type enzyme and instead expressed a mutant human enzyme [27]. The same strategy will be used to confirm EEA of NOV and related compounds in whole animals, and to determine which compound works best as a pharmacological chaperone for mutant β-Glu.

Acknowledgements

We thank Kaneski C. and Brady R.O. for human GD fibroblasts with N370S homozygous mutations (DMN00.41 and DMN87.30) and Tsuji S. for human β-Glu cDNA.

References

[1] E. Beutler, G.A. Grabowski, Gaucher disease. The Metabolic and Molecular Bases of Inherited Disease, McGraw-Hill, New York, 2001, pp. 2641–2670.
[2] N.W. Barton, R.O. Brady, J.M. Dambrosia, A.M. Di Bisceglie, S.H. Doppelt, S.C. Hill, H.J. Mankin, G.J. Murray, R.I. Parker, C.E. Argoff, et al., Replacement therapy for inherited enzyme deficiency-macrophage-targeted glucocerebrosidase for Gaucher's disease, N. Engl. J. Med. 324 (1991) 1464–1470.
[3] T. Cox, R. Lachmann, C. Hollak, J. Aerts, S. van Weely, M. Hrebicek, F. Platt, T. Butters, R. Dwek, C. Moyses, et al., Novel oral treatment of Gaucher's disease with *N*-butyldeoxynojirimycin (OGT918) to decrease substrate biosynthesis, Lancet 355 (2000) 1481–1485.
[4] G.A. Grabowski, N. Leslie, R. Wenstrup, Enzyme therapy for Gaucher disease: the first 5 years, Blood Rev. 12 (1998) 115–133.
[5] A. Erikson, H. Forsberg, M. Nilsson, M. Astrom, J.E. Mansson, Ten years' experience of enzyme infusion therapy of Norrbottnian (type 3) Gaucher disease, Acta Paediatr. 95 (2006) 312–317.
[6] F.M. Platt, M. Jeyakumar, U. Andersson, D.A. Priestman, R.A. Dwek, T.D. Butters, Inhibition of substrate synthesis as a strategy for glycolipids lysosomal storage disease therapy, J. Inherit. Metab. Dis. 24 (2001) 275–290.
[7] R. Schiffmann, M.P. Heyes, J.M. Aerts, J.M. Dambrosia, M.C. Patterson, T. DeGraba, C.C. Parker, G.C. Zirzow, K. Oliver, G. Tedeschi, et al., Prospective study of neurological responses to treatment with macrophage-targeted glucocerebrosidase in patients with type 3 Gaucher's disease, Ann. Neurol. 42 (1997) 613–621.
[8] C.A. Prows, N. Sanchez, C. Daugherty, G.A. Grabowski, Gaucher disease: enzyme therapy in the acute neuronopathic variant, Am. J. Med. Genet. 71 (1997) 16–21.
[9] M. Aoki, Y. Takahashi, Y. Miwa, S. Iida, K. Sukegawa, T. Horai, T. Orii, N. Kondo, Improvement of neurological symptoms by enzyme replacement therapy for Gaucher disease type IIIb, Eur. J. Pediatr. 160 (2001) 63–64.
[10] J.M. Aerts, C.E. Hollak, R.G. Boot, J.E. Groener, M. Maas, Substrate reduction therapy of glycosphingolipid storage disorders, Inherit. Metab. Dis. 29 (2006) 449–456.
[11] I. Ron, M. Horowitz, ER retention and degradation as the molecular basis underlying Gaucher disease heterogeneity, Hum. Mol. Genet. 14 (2005) 2387–2398.
[12] M. Schmitz, M. Alfalah, J.M. Aerts, H.Y. Naim, K.P. Zimmer, Impaired trafficking of mutants of lysosomal glucocerebrosidase in Gaucher's disease, Int. J. Biochem. Cell Biol. 37 (2005) 2310–2320.
[13] A.R. Sawkar, W. D'Haeze, J.W. Kelly, Therapeutic strategies to ameliorate lysosomal storage disorders—A focus on Gaucher disease, Cell. Mol. Life Sci. 63 (2006) 1179–1192.
[14] R.J. Desnick, E.H. Schuchman, Enzyme replacement and enhancement therapies: lessons from lysosomal disorders, Nat. Rev., Genet. 3 (2002) 954–966.
[15] H. Lin, Y. Sugimoto, Y. Ohsaki, H. Ninomiya, A. Oka, M. Taniguchi, H. Ida, Y. Eto, S. Ogawa, Y. Matsuzaki, et al., *N*-Octyl-β-valienamine up-regulates activity of F213I mutant β-glucosidase in cultured cells: a potential chemical chaperone therapy for Gaucher disease, Biochim. Biophys. Acta 1689 (2004) 219–228.
[16] A.R. Sawkar, W.C. Cheng, E. Beutler, C.H. Wong, W.E. Balch, J.W. Kelly, Chemical chaperones increase the cellular activity of N370S β-glucosidase: a therapeutic strategy for Gaucher disease, Proc. Natl. Acad. Sci. U. S. A. 99 (2002) 15428–15433.
[17] A.R. Sawkar, S.L. Adamski-Werner, W.C. Cheng, C.H. Wong, E. Beutler, K.P. Zimmer, J.W. Kelly, Gaucher disease-associated glucocerebrosidases show mutation-dependent chemical chaperoning profiles, Chem. Biol. 12 (2005) 1235–1244.
[18] V. Bernier, M. Lagace, D.G. Bichet, M. Bouvier, Pharmacological chaperones: potential treatment for conformational diseases, Trends Endocrinol. Metab. 15 (2004) 222–228.
[19] Y. Eto, H. Ida, Clinical and molecular characteristics of Japanese Gaucher disease, Neurochem. Res. 24 (1999) 207–211.
[20] A.M. Vaccaro, M. Muscillo, M. Tatti, R. Salvioli, E. Gallozzi, K. Suzuki, Effect of a heat-stable factor in human placenta on glucosylceramidase, glucosylsphingosine glucosyl hydrolase, and acid β-glucosidase activities, Clin. Biochem. 20 (1987) 429–433.
[21] F.E. Cohen, J.W. Kelly, Therapeutic approaches to protein-misfolding diseases, Nature 426 (2003) 905–909.
[22] J.Q. Fan, S. Ishii, N. Asano, Y. Suzuki, Accelerated transport and maturation of lysosomeal α-galactosidase A in Fabry lymphoblasts by an enzyme inhibitor, Nat. Med. 5 (1999) 112–115.
[23] S. Ogawa, M. Ashiura, C. Uchida, S. Watanabe, C. Yamazaki, K. Yamagishi, J. Inokuchi, Synthesis of potent β-D-glucocerebrosidase inhibitors: *N*-alkyl-β-valienamines, Bioorg. Med. Chem. Lett. 6 (1996) 929–932.
[24] S. Ogawa, Y. Kobayashi, K. Kabayama, M. Jimbo, J. Inokuchi, Chemical modification of β-glucocerebrosidase inhibitor *N*-octyl-β-valienamine: synthesis and biological evaluation of *N*-alkanoyl and *N*-alkyl derivatives, Bioorg. Med. Chem. 6 (1998) 1955–1962.
[25] K.P. Zimmer, P. le Coutre, H.M. Aerts, K. Harzer, M. Fukuda, J.S. O'Brien, H.Y. Naim, Intracellular transport of acid β-glucosidase and lysosome-associated membrane proteins is affected in Gaucher's disease (G202R mutation), J. Pathol. 188 (1999) 407–414.
[26] H. Dvir, M. Harel, A.A. McCarthy, L. Toker, I. Silman, A.H. Futerman, J.L. Sussman, X-ray structure of human acid-beta-glucosidase, the defective enzyme in Gaucher disease, EMBO Rep. 4 (2003) 704–709.
[27] J. Matsuda, O. Suzuki, A. Oshima, Y. Yamamoto, A. Noguchi, K. Takimoto, M. Itoh, Y. Matsuzaki, Y. Yasuda, S. Ogawa, et al., Chemical chaperone therapy for brain pathology in G(M1)-gangliosidosis, Proc. Natl. Acad. Sci. U. S. A. (2003) 15912–15917.

ELSEVIER

Journal of the Neurological Sciences 252 (2007) 181 – 184

Journal of the Neurological Sciences

www.elsevier.com/locate/jns

Short communication

Dopaminergic neuronal dysfunction associated with parkinsonism in both a Gaucher disease patient and a carrier

Satoshi Kono [a,*], Kentaro Shirakawa [a], Yasuomi Ouchi [b], Masanobu Sakamoto [b], Hiroyuki Ida [c], Takeshi Sugiura [a], Hiroyuki Tomiyama [d], Hitoshi Suzuki [a], Yoshitomo Takahashi [a], Hiroaki Miyajima [a], Nobutaka Hattori [d], Yoshikuni Mizuno [d]

[a] *First Department of Medicine, Hamamatsu University School of Medicine, 1-20-1 Handayama, Hamamatsu 431-3192, Japan*
[b] *Department of Neurology, Positron Medical Center, Hamamatsu Medical Center, Hamamatsu, Japan*
[c] *Department of Pediatrics, Jikei University School of Medicine, Tokyo, Japan*
[d] *Department of Neurology, Juntendo University School of Medicine, Tokyo, Japan*

Received 8 September 2006; received in revised form 23 October 2006; accepted 30 October 2006
Available online 19 December 2006

Abstract

A clinical association between Gaucher disease and parkinsonism has been demonstrated. We herein report a Japanese patient with type 3 Gaucher disease who was compound heterozygous for F213I and L444P mutations in the glucocerebrosidase gene while his father was heterozygous for the L444P mutation. They both presented with parkinsonism characterized by a predominance of akinetic-rigid signs and a favorable response to anti-Parkinson therapies. We investigated the dopaminergic neuronal function using positron emission tomography (PET) with radioligands, [^{11}C] CFT and [^{11}C] raclopride. PET studies of both patients demonstrated the [^{11}C] CFT uptake to be severely decreased in the putamen and the caudate nucleus, however, the [^{11}C] raclopride uptake was normal in the basal ganglia. Although the majority of Gaucher disease patients with parkinsonism tend to be refractory to anti-Parkinson therapies. The clinical features and the findings of the PET studies suggest that patients with parkinsonism associated with the mutation in the glucocerebrosidase gene, even in heterozygosis, may be related to the presynaptic dopaminergic neuronal dysfunction reported in Parkinson's disease. A PET study to evaluate the dopaminergic neuronal function in Gaucher disease would provide both a better understanding of the effects of anti-Parkinson therapies and a help to improve our ability to make an early diagnosis of parkinsonism associated with Gaucher disease.

Keywords: Gaucher disease; Parkinsonism; Glucocerebrosidase; PET

1. Introduction

Gaucher disease is an autosomal recessive lysosomal disorder resulting from a deficiency of the lysosomal enzyme glucocerebrosidase which lead to the systemic storage of glycosphingolipids [1]. This disease is caused by mutations in the glucocerebrosidase gene located on1q21. Recent studies have revealed an association between Gaucher disease and Parkinson's disease due to a concurrence of type 1 Gaucher disease and parkinsonism and the identification of glucocerebrosidase mutations in patients with sporadic Parkinson's disease [2–7]. Initial studies of the patients affected from Gaucher disease with the parkinsonism showed that the parkinsonism was characterized by an early onset and it tended to be refractory to levodopa therapy [2,3,5], however, there is an increasing number of reports which showed parkinsonism to demonstrate the following signs of typical Parkinson disease: namely, the asymmetric onset of rigidity, resting tremor, bradykinesia, and a favorable response to Parkinson therapies [4,8]. Treatment-refractory parkinsonism suggests that mutations in the glucocerebrosidase gene may affect either postsynaptic dopaminergic neurons or both post- and presynaptic dopaminergic neurons.

* Corresponding author. Tel.: +81 53 435 2261; fax: +81 53 434 9447.
E-mail address: satokono@hama-med.ac.jp (S. Kono).

0022-510X/$ - see front matter © 2006 Elsevier B.V. All rights reserved.
doi:10.1016/j.jns.2006.10.019

We herein investigated the dopaminergic neuronal function of the parkinsonism, responsive to levodopa therapy, in a type 3 Gaucher disease patient and his father using positron emission tomography (PET) and thus showed that our cases were involved in presynaptic dopaminergic function seen in Parkinson's disease.

2. Clinical reports

A 38-year-old Japanese man complained of difficulty in walking and a reduced speed in the normal activities of daily life. He was found to have hepatosplenomegaly at the age 6. A bone marrow analysis revealed a marked accumulation of Gaucher's cells and his glucocerebrosidase activity level was 1.8 nmol/h/mg protein (control level; 4.1–9.6 nmol/h/mg protein). He developed a generalized tonic–clonic seizure with abnormal electroencephalogram patterns at age 7 and thus was treated with anti-convulsant therapy. A neurological examination at the age 7 slowed horizontal saccadic eye movements characteristic of type 3 Gaucher disease. He was diagnosed to have type 3 Gaucher disease and thus underwent a splenectomy in early adolescence. He also suffered from spinal bone pain and abdominal pain associated with hepatomegaly at the age 28. After the initiation of enzyme replacement therapy at the age 33, the hepatomegaly and the bone pain both were improved, however, the patient gradually developed a clumsy left hand, start hesitation and freezing of gait during turning. He was unable to walk without assistance by the age 37 and thereafter presented at our hospital. His family history revealed no consanguinity and no history of Gaucher disease. A neurological examination revealed that he showed severe akinesia with a tendency to show trunk deviation to the left in the sitting position and he was unable to get up from a chair without help. He walked with a flexed posture, with small and irregular steps, while demonstrating start and turn hesitation and a reduction in his arm swing. Slurred speech, hypophonia, micrographia and generalized rigidity were also observed, as well as slowed horizontal saccadic eye movements. All other neurological examinations were unremarkable; in particular involuntary movement including tremors, and muscle strength, stretch and cutaneous plantar reflexes, co-ordination, sensory functions, or fundi and other cranial nerves were normal. A mental examination showed him to be inert. Spatial abilities were intact. His digit span was six forward, and four backward. He could repeat a seven-item name and address immediately after its oral presentation and could recall 6 of 7 items after a 5-minute delay. The Wechsler Adult Intelligence Scale (WAIS) showed verbal IQ of 60, performance IQ of 53, and full scale IQ of 52His Mini Mental State Examination (MMSE) score was 26. An electroencephalogram showed some sharp waves or spike and wave complexes over both parietal-occipital regions and abundant generalized discharges of spikes, polyspikes and slow wave complexes. Magnetic resonance imaging showed no abnormality in the brain. A slit-lamp examination and laboratory studies including thyroid function tests, serum copper and ceruloplasmin were all normal. The study of an auditory brainstem response in this patient showed no deterioration.

His 71-year-old father presented to our hospital in order to help his son. He also became aware of progressive difficulty of slowness during walking and developed a left clumsy hand at the age of 63. A neurological examination showed bradykinesia, symmetrical cogwheel rigidity of the upper limbs and poor backward postural reflexes. His sense of touch, vibration, position and cognitive abilities were intact. Her 65-year-old mother was asymptomatic. A neurological examination was unremarkable.

After PET studies of the proband and his farther, anti-Parkinson therapies including levodopa/carbidopa, cabergoline and selegeline HCl were initiated. The parkinsonian features in both patients showed a favorable response to the medication. The patient was able to walk without assistance and showed an improvement in both akinesia and rigidity. The Unified Parkinson disease rating scale (UPDRS) III motor score in the proband improved from 45 to 28. His father also improved from 23 to 16. During the follow-up, the proband showed a gradual appearance of a wearing-off phenomenon, motor fluctuations and levodopa-induced dyskinesia.

3. Methods and results

3.1. Molecular genetic analysis

Genomic DNA samples isolated from blood samples were subjected to restriction fragment length polymorphism (RFLP) analyses to identify any mutations in the glucocerebrosidase gene by a previous described method [9] For a molecular genetic analysis for hereditary Parkinson disease, the sequencing of the gene for α-synuclein and parkin was performed by a previously reported technique [10,11]. The genetic study demonstrated that the proband carried two known missence mutations in the glucocerebrosidase gene, L444P in exon 10 and F213I in exon 6 (Fig. 1A). The RFLP analyses of his father demonstrated a L444P mutation on the paternal allele. No mutations in the α-synuclein gene or the parkin gene were identified in the proband and his father.

3.2. PET scan

PET was performed by a high-resolution brain PET scanner (SHR12000, Hamamatsu Photonics K.K., Hamamatsu, Japan). The head of a patient was fixated using a thermoplastic face-mask enabling to fix it to the same place between separate PET measurements. First, 72 min after a bolus intravenous injection of the [^{11}C] CFT, 20-minute PET data were collected to produce a late-phase image of [^{11}C] CFT uptake [12]. Next, following three hours to allow for a decay of [^{11}C] CFT radioactivity, the same patient were scanned for 62 min after [^{11}C] raclopride injection using a

serial scans protocol [13] The final PET images were generated as semi-quantitative parametric images (a standardized uptake value image for [^{11}C] CFT, and a distribution image for [^{11}C] raclopride). Based on the regions of interest (ROIs) method, we placed the ROIs on the caudate nucleus, putamen and cerebellum on the MR images, and then transferred them onto the corresponding PET images, and finally calculated a semi-quantitative striatum/cerebellum ratio by dividing the ROI counts of either the caudate nucleus or the putamen by cerebellar counterparts. The ratio from a patient and his father was compared with the ratios from three normal control subjects and assessed statistically

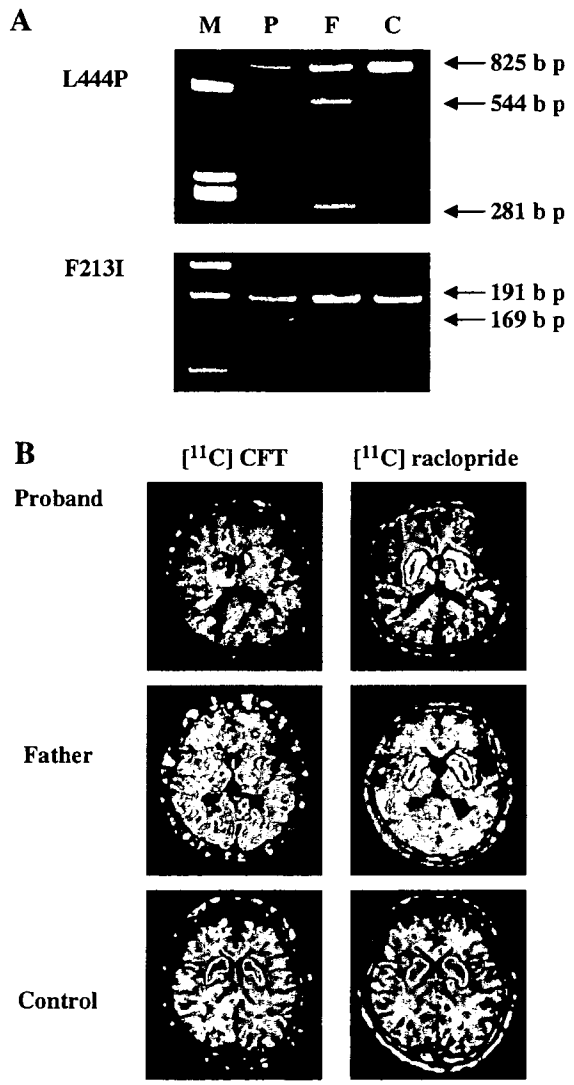

Fig. 1. A. Restriction fragment length polymorphism analyses of the L444P and the F213I mutation in the patient and his father. When the L444P mutation is present, restriction enzyme (NclI) digests an 825 bp PCR product, thus producing two fragments of 544 bp and 281 bp. When the F213I mutation is present, a restriction enzyme (AseI) digests a 191 bp PCR thereby producing two fragments of 169 bp and 22 bp M: molecular marker, P: patient, F: patient's father, C: control. B. Transaxial PET slices blended with MRI images of the proband, his father and a 38-year-old healthy man as a control.

Table 1

	Patient	His father	Normal subjects (n=3) (mean±S.D.)
[^{11}C] CFT			
Caudate nucleus/cerebellum ratio	1.82	1.56	3.83±0.07
Putamen/cerebellum ratio	1.42	1.37	3.90±0.13
[^{11}C] raclopride			
Caudate nucleus/cerebellum ratio	3.93	3.72	4.33±0.13
Putamen/cerebellum ratio	4.02	4.14	4.49±0.31

The uptake of [^{11}C] CFT in the both putamen and caudate nucleus was significantly reduced at $p<0.05$ by one sample t-test.

by one sample t-test (Table 1). The PET images of the patient and his father showed similar results. The uptake of [^{11}C] CFT in the both putamen and caudate nucleus was significantly reduced ($p<0.05$), while the [^{11}C] raclopride uptake showed a relative decrease in the same striatal regions in comparison with normal counterparts.

4. Discussion

This report documented fascinating clinical and PET findings in two patients with the same family lineage who both developed parkinsonism. The clinical features of our cases are as follows; 1) the proband with type 3 Gaucher disease and his father developed parkinsonism, 2) molecular genetic analyses in the glucocerebrosidase gene showed the proband to be compound heterozygous for L444P and F213I, while his father is heterozygous for the L444P mutation, 3) the parkinsonism showed a favorable response to anti-Parkinson therapies and 4) a dopaminergic functional neuroimaging study of both patients showed a presynaptic dopaminergic dysfunction which is normally seen in Parkinson's disease patients. Parkinsonism has been described as a rare neurological phenotype of patients with type 1 Gaucher disease [2,3] The parkinsonism in such patients is characteristically early-onset and most tend to show a poor response to levodopa therapy. The enzyme replacement therapy is not effective for the treatment of the parkinsonism in such cases. The neuropathological findings characteristic to Gaucher disease with parkinsonism showed a marked loss of dopaminergic neurons in the substantia nigra, synuclein-positive Lewy bodies and the involvement of hippocampal CA2-4 regions where glucocerebrosidase was expressed [5,14]. While the concurrence of Gaucher disease and parkinsonism could still be coincidental, the shared clinical characteristics and neuropathology of previous case reports suggest a related etiology. In our proband the diagnosis of Gaucher disease was firmly established both by a deficiency in the glucocerebrosidase activity and the gene analysis in the glucocerebrosidase gene. The first clinical manifestations including hepatosplenomegaly, slow saccadic eye movements and epilepsy preceded by osseous pain, appearing in adulthood, suggest our case to have type 3 Gaucher disease The L444P and the F213I mutations identified in our patients

are frequent in patients affected with both type 1 and 2 as well as type 3 Gaucher disease [1,9]. Although the correlation between genotypes and phenotypes in Gaucher disease is investigated, the conclusion remains elusive [1] Although many reports have demonstrated a clinical association between type 1 Gaucher disease and parkinsonism, type 3 Gaucher disease with parkinsonism is uncommon. The proband appeared to have early-onset parkinsonism which developed in his 30's as previous reports in type 1 Gaucher disease patients with parkinsonism [5]. The patient's father who carried the L444P allele developed parkinsonism in his 60's. A recent study demonstrates that parkinsonism appears to be associated with heterozygosity for a mutation in the glucocerebrosidase gene [8]. This observation indicates that the L444P mutation found in the father, even in heterozygotes, may thus be a risk factor for the development of parkinsonism. The correlation between parkinsonism as a phenotype and mutations in the glucocerebrosidase gene as a genotype has not yet been established. N370S, L444P, 84GG mutations are reported as common mutations associated with parkinsonism in Gaucher disease patients and their carriers, however, it is evident that the majority of the patients or carriers with such mutations do not always develop parkinsonism [4,5,8] An intriguing clinical feature of our patients was the fact that they had treatment-responsive parkinsonism, because initial case reports showed the parkinsonian symptoms in Gaucher disease patients to be refractory to levodopa therapy [2,3,5]. In addition, the association between a favorable response to L-Dopa and the mutation in patients with Gaucher disease has been reported in some studies. Bembi et al. reported 4 cases with a good response to L-Dopa who had either N370S, L444P or G337S mutation [4]. Goker-Alpan et al. also showed some cases with a good response to L-Dopa therapy and they had either N370S or L444P mutations, however, not all the patients with such a mutation always showed an effective response to L-Dopa therapy [8].

We evaluated the dopaminergic function of our patients using neuroimaging techniques with a PET system [^{11}C] CFT, a dopamine transporter probe, allows us to study the integrity of the presynaptic dopaminergic system [12]. [^{11}C] raclopride, a low affinity dopaminergic D2 receptor ligand, has been used to study the post synaptic dopaminergic function [13]. The PET study with the combined use of [^{11}C] CFT and [^{11}C] raclopride in our patients who both carried the L444P mutation allele showed a presynaptic dopaminergic dysfunction The mutation in the glucocerebrosidase gene, even in heterozygosis, may be associated with the presynaptic dopaminergic neuronal dysfunction which shares a common pathogenesis to Parkinson's disease. It is not clear why the parkinsonism associated with mutations in the glucocerebrosidase gene shows such variation in the responsiveness to levodopa therapy. We speculate that at the onset of the parkinsonism, this mutation may be associated with a dysfunction of presynaptic dopaminergic neuron and then, during the progression of the parkinsonism, the patient may develop dysfunction of postsynaptic dopaminergic neurons resulting in the poor responsiveness to levodopa therapy. Another possibility may be that other genetic or environmental factors may interact with the glucocerebrosidase gene thus resulting in the development of variation in the responsiveness to anti-Parkinson therapy. It is important to be aware of the association between Gaucher disease and parkinsonism. We should therefore investigate parkinsonian symptoms in not only probands of Gaucher disease but also their family members. A PET study to evaluate pre- and postsynaptic dopaminergic neuronal function provides an excellent understanding of an association with Gaucher disease and Parkinson's disease.

References

[1] Sidransky E. Gaucher disease: complexity in a "simple" disorder. Mol Genet Metab 2004;83:6–15.
[2] Neudorfer O, Giladi N, Elstein D, Abrahamov A, Turezkite T, Aghai E, et al. Occurrence of Parkinson's syndrome in type I Gaucher disease. QJM 1996;89:691–4.
[3] Varkonyi J, Simon Z, Soos K, Poros A. Gaucher disease type I complicated with Parkinson's syndrome. Haematologia (Budap) 2002;32:271–5.
[4] Bembi B, Zambito Marsala S, Sidransky E, Ciana G, Carrozzi M, Zorzon M, et al. Gaucher's disease with Parkinson's disease: clinical and pathological aspects. Neurology 2003;61:99–101.
[5] Tayebi N, Walker J, Stubblefield B, Orvisky E, LaMarca ME, Wong K, et al. Gaucher disease with parkinsonian manifestations: does glucocerebrosidase deficiency contribute to a vulnerability to parkinsonism? Mol Genet Metab 2003;79:104–9.
[6] Aharon-Peretz J, Rosenbaum H, Gershoni-Baruch R. Mutations in the glucocerebrosidase gene and Parkinson's disease in Ashkenazi Jews. N Engl J Med 2004;351:1972–7.
[7] Zimran A, Neudorfer O, Elstein D. The glucocerebrosidase gene and Parkinson's disease in Ashkenazi Jews. N Engl J Med 2005;352:728–31 [author reply 728-31].
[8] Goker-Alpan O, Schiffmann R, LaMarca ME, Nussbaum RL, McInerney-Leo A, Sidransky E. Parkinsonism among Gaucher disease carriers. J Med Genet 2004;41:937–40.
[9] Ida H, Rennert OM, Kawame H, Ito T, Maekawa K, Eto Y. Mutation screening of 17 Japanese patients with neuropathic Gaucher disease. Hum Genet 1996;98:167–71.
[10] Kitada T, Asakawa S, Hattori N, Matsumine H, Yamamura Y, Minoshima S, et al. Mutations in the parkin gene cause autosomal recessive juvenile parkinsonism. Nature 1998;392:605–8.
[11] Chan P, Jiang X, Forno LS, Di Monte DA, Tanner CM, Langston JW. Absence of mutations in the coding region of the alpha-synuclein gene in pathologically proven Parkinson's disease. Neurology 1998;50:1136–7.
[12] Ouchi Y, Kanno T, Okada H, Yoshikawa E, Futatsubashi M, Nobezawa S, et al. Changes in dopamine availability in the nigrostriatal and mesocortical dopaminergic systems by gait in Parkinson's disease. Brain 2001;124:784–92.
[13] Ouchi Y, Yoshikawa E, Futatsubashi M, Okada H, Torizuka T, Sakamoto M. Effect of simple motor performance on regional dopamine release in the striatum in Parkinson disease patients and healthy subjects: a positron emission tomography study. J Cereb Blood Flow Metab 2002;22:746–52.
[14] Wong K, Sidransky E, Verma A, Mixon T, Sandberg GD, Wakefield LK, et al. Neuropathology provides clues to the pathophysiology of Gaucher disease. Mol Genet Metab 2004;82:192–207.

International Journal of
HEMATOLOGY

Case Report

Pseudo–Gaucher Cell Proliferation Associated with Myelodysplastic Syndrome

Takeshi Saito,[a] Noriko Usui,[a] Osamu Asai,[a] Nobuaki Dobashi,[a] Hiroyuki Ida,[b] Makio Kawakami,[c] Shingo Yano,[a] Hiroshi Osawa,[a] Yutaka Takei,[a] Shinobu Takahara,[a] Yoji Ogasawara,[a] Yuko Yamaguchi,[a] Jiro Minami,[a] Keisuke Aiba[a]

[a]*Division of Oncology and Hematology, Department of Internal Medicine, Jikei University School of Medicine, Tokyo, Japan;* [b]*Department of Pediatrics, Jikei University School of Medicine, Tokyo, Japan;* [c]*Department of Pathology, Jikei University School of Medicine, Tokyo, Japan*

Received July 21, 2006; received in revised form December 6, 2006; accepted February 2, 2007

Abstract

We report an extremely rare case of pseudo–Gaucher cell proliferation with myelodysplastic syndrome (MDS). A 77-year-old Japanese man was referred to our hospital with splenomegaly and thrombocytopenia, and subsequent bone marrow aspiration revealed infiltrates of foamy vacuolated macrophages without any evidence of other morphologic abnormalities. A karyotype analysis showed the presence of 46,XY,del(20)(q11) in 20 of 20 examined bone marrow cells. We performed a splenectomy, and the resulting pathologic findings revealed massive infiltration of foamy vacuolated macrophages, which were morphologically compatible with Gaucher cells. The activities of β-glucosidase and acid sphingomyelinase were within normal ranges; therefore, the foamy vacuolated macrophages were considered pseudo–Gaucher cells. A diagnosis of MDS, subclassified as refractory anemia, was then made according to World Health Organization classification guidelines. Pseudo–Gaucher cell proliferation and infiltration might therefore be observed in other patients presenting with MDS.
Int J Hematol. 2007;85:350-353. doi: 10.1532/IJH97.06153

Key words: MDS; Pseudo–Gaucher cell; Splenomegaly; Macrophage

1. Introduction

The Gaucher cell is the pathologic hallmark of Gaucher disease, which is caused by a congenital deficiency of β-glucocerebrosidase. The resulting accumulation of glucocerebroside deposits in the cytoplasm of histiocytes in patients with Gaucher disease leads to the formation of foamy vacuolated macrophages. Pseudo–Gaucher cells, which are macrophages with a cytoplasm containing needle-like and foamy inclusions resembling those of Gaucher cells [1], have occasionally been described in various hematologic malignancies, including chronic myeloid leukemia [2], malignant lymphoma [3], and multiple myeloma [4]. We report an extremely rare case of myelodysplastic syndrome (MDS) with splenomegaly related to massive infiltration by pseudo–Gaucher cells.

Correspondence and reprint requests: Takeshi Saito, MD, Division of Oncology and Hematology, Department of Internal Medicine, Jikei University School of Medicine, 19-18 Nishishinbashi 3-chome, Minato-ku, Tokyo 105-8461, Japan; fax: 81-3-3578-9753 (e-mail: takexsaito@aol.com).

2. Case Report

A 77-year-old Japanese man was referred to our hospital in December 2004 because of splenomegaly and a bleeding tendency. His family history was negative for splenomegaly and metabolic diseases. Our physical examinations revealed giant splenomegaly (12 cm below the costal margin), and an abdominal computed tomography scan further revealed a homogeneous enlargement of the spleen without parenchymal lesions (Figure 1A). Galium 67 scintigraphy revealed abnormal accumulation of this isotope in the spleen (Figure 1B). Laboratory findings are shown in Table 1. Neurologic examinations revealed no abnormality, and peripheral blood examinations showed the following: white blood cell count, 3.6×10^9/L (47.8% neutrophils, 26.4% lymphocytes, 16.9% monocytes, 8.1% eosinophils); hemoglobin, 13.3 g/dL; hematocrit, 41.6%; platelet count, 22×10^9/L. A blood chemistry analysis revealed the following: total bilirubin, 0.9 mg/dL; aspartate aminotransferase, 12 U/L; alanine aminotransferase, 15 U/L; lactate dehy-

drogenase, 142 U/L; alkaline phosphatase, 162 U/L; ferritin, 41.9 ng/mL; immunoglobulin G (IgG), 1217 mg/dL; IgA, 79 mg/dL; IgM, 92 mg/dL; soluble interleukin 2 receptor, 622 U/mL. The results of a complete serologic workup for infections, including infection by human immunodeficiency virus, hepatitis B virus, and hepatitis C virus, were negative. Epstein-Barr virus DNA and cytomegalovirus antigen in the plasma (C7-HRP test) were also undetectable. A bone marrow aspirate showed a slightly hyperplastic marrow with small numbers (3.2%) of foamy vacuolated macrophages (Figure 2). Other morphologic abnormalities were not found, except for erythroid dysplasia (Figure 3). In addition, a karyotype analysis showed the chromosomal abnormality 46,XY,del(20)(q11) in 20 of 20 examined bone marrow cells. No manifestations of bone marrow fibrosis or osteosclerosis were noted in specimens of the bone marrow biopsy.

At this stage of our examination, we could not rule out hematologic malignancies, chronic myeloproliferative disorders, and metabolic disorders such as Gaucher disease or Niemann-Pick disease. Hence, we performed a splenectomy in January 2005 to confirm the diagnosis, and a pathologic examination of the spleen showed massive infiltration of foamy vacuolated macrophages, which were morphologically compatible with Gaucher cells (Figure 4). Extramedullary hematopoiesis was not observed in the spleen. These morphologic findings prompted us to measure the activities of β-glucosidase and acid liposomal sphingomyelinase, which were within the normal ranges (378 nmol/mg per hour and 43.3 nmol/mg per hour, respectively). We therefore concluded that the foamy vacuolated macrophages we observed were pseudo–Gaucher cells. We subsequently made a diagnosis of MDS, subclassified as refractory anemia, according to World Health Organization classification criteria. After splenectomy, the patient's platelet count increased to greater than 80×10^9/L. No other complications, such as hepatomegaly, opportunistic infection, and MDS progression, were observed.

Table 1.
Laboratory Data*

Peripheral blood		Bone marrow	
White blood cells	3.6×10^9/L	Nucleated cell count	210×10^3/μL
Blasts	0%	Megakaryocytes	0/μL
Myelocytes	0%	Myeloid/erythroid ratio	0.97
Neutrophils	47.8%	Blasts	2.8%
Eosinophils	8.1%	Promyelocytes	6%
Basophils	0.8%	Myelocytes	14.4%
Lymphocytes	26.4%	Metamyelocytes	5.2%
Monocytes†	16.9%	Band neutrophils	8.8%
Red blood cells	466×10^4/μL	Segmented neutrophils	3.2%
Hemoglobin	13.3 g/dL	Eosinophils	4%
Hematocrit	41.6%	Basophils	0.8%
Platelets	22×10^9/L	Monocytes	0.4%
Coagulation		Lymphocytes	5.2%
Prothrombin time	71%	Plasma	0.4%
Activated partial thromboplastin time	35.6 s	Macrophages‡	3.2%
Fibrinogen	231 mg/dL	Erythroblasts§	45.6%
Biochemical tests		Ringed sideroblasts	0%
Total protein	6.4 g/dL	Molecular analyses	
Albumin	4.3 g/dL	BCR/ABL (PCR)	(–)
Total bilirubin	0.9 mg/dL	EBV DNA (PCR)	(–)
Aspartate aminotransferase	12 U/L		
Alanine aminotransferase	15 U/L	Infection	
Lactate dehydrogenase	142 U/L	HIV	(–)
Alkaline phosphatase	162 U/L	HTLV-I	(–)
γ-Glutamyl transpeptidase	28 U/L	HBV	(–)
Blood urea nitrogen	32 mg/dL	HCV	(–)
Creatinine	1.2 mg/dL		
Sodium	145 mEq/L	Others	
Potassium	9.6 mEq/L	Soluble interleukin 2 receptor	622 nmd/mg/hr
Chloride	107 mEq/L	β-Glucosidase	378 nmol/mg/hr
C-reactive protein	0.32 mg/dL	Acid liposomal sphingomyelinase	43.3 nmol/mg/hr
Ferritin	41.9 ng/mL		
IgG	1217 mg/dL		
IgA	79 mg/dL		
IgM	92 mg/dL		

*PCR indicates polymerase chain reaction analysis; EBV, Epstein-Barr virus; HIV, human immunodeficiency virus; HTLV-I, human T-cell lymphotropic virus I; HCV, hepatitis C virus; HBV, hepatitis B virus; IgG, immunoglobulin G.

†These monocytes have no morphologic abnormality.

‡The macrophages are pseudo–Gaucher cells.

§These erythroblasts exhibit a mild dysplastic change.

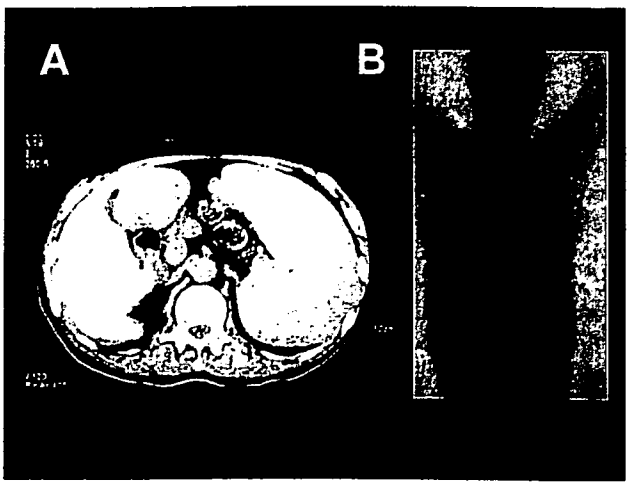

Figure 1. Computed tomography scan showing a markedly enlarged spleen (A). Galium 67 accumulation in the spleen (B).

3. Discussion

Gaucher disease is characterized by an abnormal accumulation of glucocerebroside in cells of the monocyte-macrophage system of the liver, spleen, bone marrow, and central nervous system. A diagnosis of Gaucher disease is usually made in childhood after organomegaly and/or pancytopenia are noted, but this disorder also is occasionally found in adults as old as 70 years [5]. Typical Gaucher cells have a characteristic "wrinkled tissue paper" appearance to the cytoplasm due to glucocerebroside deposition and can be up to 60 μm in diameter. In addition, some Gaucher cells can also display tubular or fibrillary structures in the cytoplasm [6]. Pseudo–Gaucher cells are macrophages with a cytoplasm that contains needle-like or foamy inclusions, thus resembling Gaucher cells, and have been found in infectious diseases [7,8] and in hematologic malignancies such as chronic myeloid leukemia, malignant lymphoma, and multiple myeloma [2-4].

To our knowledge, few MDS cases presenting with pseudo–Gaucher cells have been reported [9,10], in contrast to the sea-blue histiocytosis complications that have commonly been noted with this disorder. The pathologic characteristics of typical sea-blue histiocytes are large macrophages that vary from 20 to 60 μm in diameter and have a single eccentric nucleus and cytoplasm packed with sea-blue-green granules [11]. In our current case study, the macrophages displayed an impressive foamy vacuolation without sea-blue granules and resembled Gaucher cells or Niemann Pick cells. Late onset of either Gaucher disease or Niemann Pick disease in this individual was excluded because β-glucocerebrosidase and acid sphingomyelinase activities were at normal levels. The foamy vacuolated macrophages in this patient were therefore diagnosed as pseudo–Gaucher cells.

An important issue that arises from this diagnosis is whether these pseudo–Gaucher cells belong to the MDS clone or are in fact normal macrophages that have become overwhelmed by the lipid load. A previous study supporting the latter theory [11] has shown that the accumulation of these cells in the spleen and bone marrow is a secondary phenomenon associated with the extensive turnover of hematopoietic cells. Under these conditions, the macrophages may be unable to fully metabolize lipids. Pseudo–Gaucher cells probably arise during MDS because of ineffective hematopoiesis that leads to the destruction of hematopoietic cells and the resulting saturation of the normal pathways that remove membrane lipids. Other investigators have reported a correlation in leukemia between the karyotypic abnormality del(20)(q11) and phagocytosis [12,13]. The genes contained in

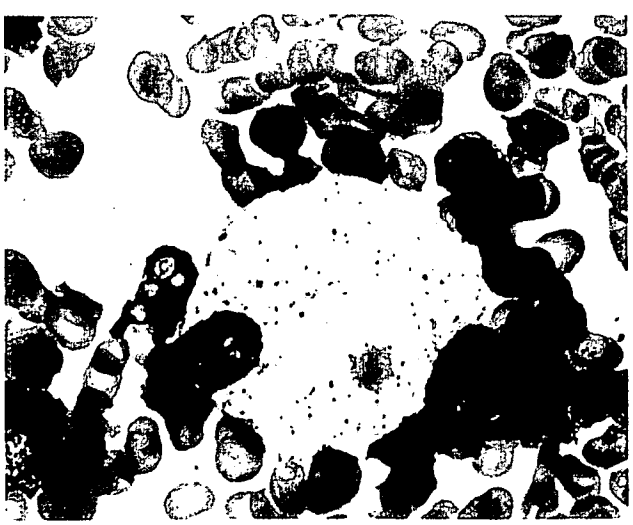

Figure 2. Pseudo–Gaucher cells in a bone marrow smear. These cells have a diameter of 30 to 60 μm and pale, abundant cytoplasm that includes foamy vacuolations and a single eccentric nucleus (May-Giemsa, original magnification ×1000).

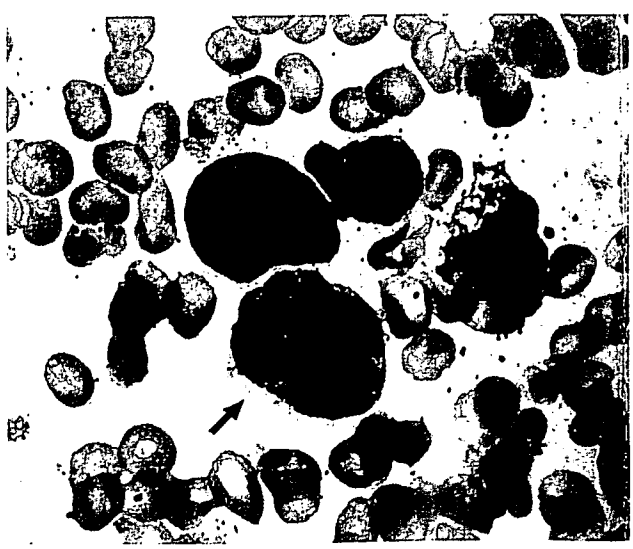

Figure 3. Evaluation of a bone marrow aspirate. Morphologic abnormalities with nuclear dysplasia were observed in erythroid cells. A multinucleate polychromatic erythroblast (arrow) can be seen (May-Giemsa, original magnification ×1000).

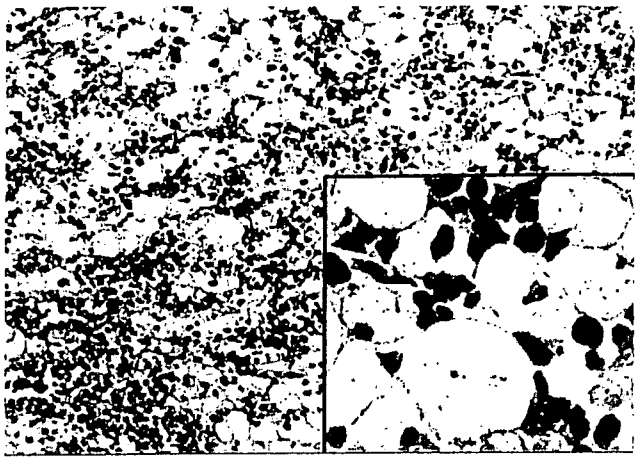

Figure 4. Evidence of pseudo–Gaucher cell infiltration in the spleen (hematoxylin-eosin, original magnification ×200 and ×1000 [inset]).

the long arm of chromosome 20 are known to include hematopoietic cell kinases [14], and some functional genes that contribute to the pathogenesis in these patients may also be present in this region. Pseudo–Gaucher cells have been suggested to belong to the MDS clone. We could not confirm this possibility in our present case study; therefore, future studies that use in situ hybridization analysis with chromosome-specific probes to examine pseudo–Gaucher cells in patients with MDS might determine whether these cells are clonal in nature.

In summary, we report an extremely rare case of a complication of pseudo–Gaucher cell proliferation associated with MDS; it is possible that this complication can be observed in additional patients with MDS. Further reporting of such cases is needed to elucidate the mechanism of pseudo–Gaucher cell proliferation, which is still unknown, and to determine whether there is any prognostic significance regarding the presence of these cells in MDS.

References

1. Carrington PA, Stevens RF, Lendon M. Pseudo-Gaucher cells. *J Clin Pathol.* 1992;45:360.
2. Busche G, Majewski H, Schlue J, et al. Frequency of pseudo-Gaucher cells in diagnostic bone marrow biopsies from patients with Ph-positive chronic myeloid leukaemia. *Virchows Arch.* 1997;430: 139-148.
3. Robak T, Urbanska-Rys H, Jerzmanowski P, Bartkowiak J, Liberski P, Kordek R. Lymphoplasmacytic lymphoma with monoclonal gammopathy-related pseudo-Gaucher cell infiltration in bone marrow and spleen: diagnostic and therapeutic dilemmas. *Leuk Lymphoma.* 2002;43:2343-2350.
4. Scullin DC Jr, Shelburne JD, Cohen HJ. Pseudo-Gaucher cells in multiple myeloma. *Am J Med.* 1979;67:347-352.
5. Grabowski GA, Andria G, Baldellou A, et al. Pediatric non-neuronopathic Gaucher disease: presentation, diagnosis and assessment: consensus statements. *Eur J Pediatr.* 2004;163:58-66.
6. Beutler E. Gaucher's disease. *N Engl J Med.* 1991;325:1354-1360.
7. Dunn P, Kuo MC, Sun CF. Pseudo-Gaucher cells in mycobacterial infection: a report of two cases. *J Clin Pathol.* 2005;58:1113-1114.
8. Abramson N. Images in hematology: Gaucher cells and HIV. *Blood.* 2006;107:11.
9. Taketomi T, Uemura K, Hara A, Saito H. Biochemical characterization of peripheral blood in an outpatient with atypical Gaucher's disease type 1 like myelodysplastic syndrome. *Jpn J Exp Med.* 1989;59:85-88.
10. Stewart AJ, Jones RDG. Pseudo-Gaucher cells in myelodysplasia. *J Clin Pathol.* 1999;52:917-918.
11. Howard MR, Kesteven PJL. Sea blue histiocytosis: a common abnormality of the bone marrow in myelodysplastic syndromes. *J Clin Pathol.* 1993;46:1030-1032.
12. Kuyama J, Fushino M, Take H, Kanayama Y. Myelodysplastic syndrome associated with erythrophagocytosis by blasts and myeloid cells. *Int J Hematol.* 1995;62:243-246.
13. Mori H, Tawara M, Yoshida Y, et al. Minimally differentiated acute myeloid leukemia (AML-M0) with extensive erythrophagocytosis and del(20)(q11) chromosome abnormality. *Leuk Res.* 2000;24:87-90.
14. Asimakopoulos FA, White NJ, Nacheva E, Green AR. Molecular analysis of chromosome 20q deletions associated with myeloproliferative disorders and myelodysplastic syndromes. *Blood.* 1994;84:3086-3094.

the FEBS Journal

MINIREVIEW

Active-site-specific chaperone therapy for Fabry disease

Yin and Yang of enzyme inhibitors

Jian-Qiang Fan[1] and Satoshi Ishii[2]

1 Department of Human Genetics, Mount Sinai School of Medicine, New York, NY, USA
2 Department of Agricultural and Life Sciences, Obihiro University of Agriculture and Veterinary Medicine, Japan

Keywords
active-site-specific chaperone; 1-deoxygalactonojirimycin; endoplasmic reticulum associated degradation; Fabry disease; α-galactosidase A; pharmacological chaperone; protein misfolding

Correspondence
J.-Q. Fan, Department of Human Genetics, Mount Sinai School of Medicine, Fifth Avenue at 100th Street, New York, NY 10029, USA
E-mail: jian-qiang.fan@mssm.edu

Declaration of interest
J.-Q. Fan and S. Ishii are coinventors of patents related to the ASSC technology which is now licensed to Amicus Therapeutics, Inc., Cranbury, NJ, USA and declare competing financial interests

(Received 8 June 2007, accepted 13 August 2007)

doi:10.1111/j.1742-4658.2007.06041.x

Protein misfolding is recognized as an important pathophysiological cause of protein deficiency in many genetic disorders. Inherited mutations can disrupt native protein folding, thereby producing proteins with misfolded conformations. These misfolded proteins are consequently retained and degraded by endoplasmic reticulum-associated degradation, although they would otherwise be catalytically fully or partially active. Active-site directed competitive inhibitors are often effective active-site-specific chaperones when they are used at subinhibitory concentrations. Active-site-specific chaperones act as a folding template in the endoplasmic reticulum to facilitate folding of mutant proteins, thereby accelerating their smooth escape from the endoplasmic reticulum-associated degradation to maintain a higher level of residual enzyme activity. In Fabry disease, degradation of mutant lysosomal α-galactosidase A caused by a large set of missense mutations was demonstrated to occur within the endoplasmic reticulum-associated degradation as a result of the misfolding of mutant proteins. 1-Deoxygalactonojirimycin is one of the most potent inhibitors of α-galactosidase A. It has also been shown to be the most effective active-site-specific chaperone at increasing residual enzyme activity in cultured fibroblasts and lymphoblasts established from Fabry patients with a variety of missense mutations. Oral administration of 1-deoxygalactonojirimycin to transgenic mice expressing human R301Q α-galactosidase A yielded higher α-galactosidase A activity in major tissues. These results indicate that 1-deoxygalactonojirimycin could be of therapeutic benefit to Fabry patients with a variety of missense mutations, and that the active-site-specific chaperone approach using functional small molecules may be broadly applicable to other lysosomal storage disorders and other protein deficiencies.

Lysosomal α-galactosidase A (α-Gal A) is responsible for the catabolism of neutral glycosphingolipids that have an α-galactose residue at their nonreducing terminus [1]. Genetic deficiency of the enzyme, which is encoded by the X-chromosome, results in Fabry disease, and leads to the progressive storage of glycosphingolipids, predominantly globotriaosylceramide, in the lysosomes of vascular endothelial cells. The disease is classified into two major phenotypes according to the onset of clinical symptoms: the early onset (or

Abbreviations
ASSC, active-site-specific chaperone; DGJ, 1-deoxygalactonojirimycin; ER, endoplasmic reticulum; ERAD, endoplasmic reticulum-associated degradation; ERT, enzyme replacement therapy; α-Gal A, α-galactosidase A.

classic) type and the late-onset (or variant) form. Clinical symptoms in classic Fabry patients are severe, and range from angiokeratomas, acroparesthesia, hypohidrosis, corneal opacity in the early teens, and progressive vascular disease of the heart, kidneys and central nervous system [2]. By contrast, patients with late-onset or variant phenotypes are usually asymptomatic until their late thirties, and their clinical manifestations are often limited to the heart [3,4] or kidneys [5]. Without medical intervention, death typically occurs in the fourth or fifth decade of life as a result of renal failure or cerebrovascular disease in classic Fabry disease [6,7], or in the fifth or sixth decade of life in variant patients who eventually suffer from heart failure or end-stage renal failure [8]. The prevalence of Fabry disease is estimated at 1 : 40 000 for the classic form. The incidence of the variant form of Fabry disease was found to be higher. Screening of various ethnic groups revealed that the incidence of cardiac variant Fabry disease among patients with unexplained hypertrophic cardiomyopathy was 3–6% [4,9], and approximately 1% of hemodialysis patients were shown to have a variant form of Fabry disease [5,10], suggesting that variant patients may be far more prevalent than previously estimated.

To date, more than 400 mutations have been identified in the α-Gal A gene *GLA* (Human Gene Mutation Database Web site, http://www.hgmd.cf.ac.uk/). More than 57% of mutations are missense, and the majority of mutations are private, occurring only in one or a few families. The correlation between genotype and residual enzyme activity (measured primarily in leukocytes) is not strong, and presumably depends upon the nature of the mutation and additional genetic or nongenetic factors. However, the correlation between residual enzyme activity and clinical manifestations has clearly been demonstrated; higher residual enzyme activities cause mild variant phenotypes, whereas mutations that result in low residual or nondetectable enzyme activities are likely to lead to the classic phenotype [11]. Therefore, an increase in even a fraction of residual enzyme activity in patients is expected to dramatically modify disease progression and improve their quality of life.

Currently, enzyme replacement therapy (ERT) is the only effective treatment for Fabry disease. Infusion of recombinant α-Gal A purified from Chinese hamster ovary cells or fibroblasts is effective in lowering the accumulation of substrate in tissues, and reduces pain in classically affected Fabry patients [12,13]. The therapy has been well tolerated by patients who revealed improvements in gastrointestinal and neurological manifestations (acroparaesthesia, hypohidrosis, and vasomotion) and quality of life [14,15]. The results of treatment of variant Fabry patients have been mixed, suggesting that ERT may be inefficient at treating severe late-stage patients, presumably because of insufficient delivery of enzyme to particular tissues [16,17]. The therapy is expensive, which could be an economic burden for patients, especially for those living in developing countries.

An emerging therapeutic strategy using small molecules termed active-site-specific chaperones (ASSC) that are 'pharmacological chaperones' has been proposed, and is being evaluated for Fabry disease [18,19]. This strategy employs orally active molecules that are able to increase residual enzyme activity by rescuing misfolded mutant proteins from endoplasmic reticulum-associated degradation (ERAD), and promoting the smooth processing and trafficking of mutant enzymes to lysosomes. In addition to Fabry disease, small molecules capable of specifically rescuing misfolded enzyme proteins have been identified for Gaucher disease [20,21], Tay-Sachs and Sandhoff disease [22] (details for Gaucher and Tay-Sachs/Sandhoff diseases are reviewed separately), GM1-gangliosidosis [23], and retinitis pigmentosa 17 [24]. Small molecular antagonists have been identified as pharmacological chaperones for rescue of conformational defective receptors, and are reviewed elsewhere [25,26]. In this review, ASSC will be used to refer to these molecules because they are active-site directed inhibitors of the targeted enzyme. Herein, we describe a molecular basis for the deficient activity of α-Gal A in mutant enzymes that are identified in Fabry patients with residual enzyme activity, and review recent progress in the development of ASSC therapy for Fabry disease. Particularly, 1-deoxygalactonojirimycin (DGJ) is explored as an example of the development of ASSC therapy.

Structural basis of Fabry disease

The mature human α-Gal A enzyme is a homodimeric glycoprotein, each monomer containing 398 amino acid residues after cleavage of the signal peptide (the first 30 amino acid residues) [27]. From X-ray crystal structural information, each monomer is composed of two domains; a $(\beta/\alpha)_8$ domain (amino acid residues 32–330), and a C-terminal domain (residues 331–429) containing eight antiparallel β strands on two sheets in a β sandwich (Fig. 1A) [28]. The first domain contains the active-site formed by the C-terminal ends of the β strands at the center of a barrel. Thirteen amino acid residues were predicted to be directly involved in the interaction with α-galactose. In addition, 30 residues from loops β1-α1, β6-α6, β7-α7, β8-α8, β11-β12, and β15-β16 of each monomer contribute

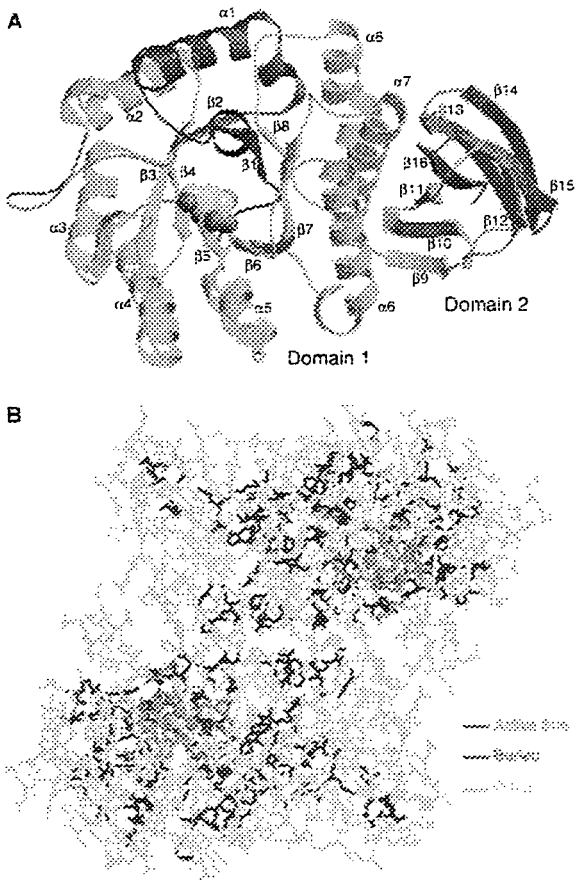

Fig. 1. Structure of the α-Gal A monomer (A) and location of Fabry disease mutations (B). (A) The monomer is colored from the N- (blue) to C- (red) terminus. Domain 1 contains the active-site at the center of the β strands in the $(\beta/\alpha)_8$ barrel, whereas domain 2 contains antiparallel β strands. The galactose ligand is shown in yellow and red. (B) Fabry disease-causing point mutations are shown on the human α-Gal A dimer. The red, blue, and green bonds show mutations that directly perturb the active-site, involve buried residues, or fall into neither of these categories, respectively. Reproduced with permission from Garman *et al.* [28].

to the dimer interface. To understand the molecular defects responsible for Fabry disease, Garman *et al.* [28,29] mapped various missense mutations onto a model of human α-Gal A (Fig. 1B). The locations of the human α-Gal A point mutations reveal two major classes of Fabry disease protein defects: active-site mutations that reduce enzymatic activity by perturbing the active site without necessarily affecting the overall α-Gal A structure; and folding mutations that reduce the stability of α-Gal A by disrupting its hydrophobic core. It is clear that the majority of amino acids that are replaced within missense mutant proteins do not directly contribute to the enzyme's catalytic function, but rather to the maintenance of the enzyme's tertiary structure.

Molecular basis of the deficiency of human mutant α-Gal A enzymes

The deficient activity of mutant α-Gal A enzymes can result from the defective biosynthesis, loss of kinetic capability, excessive degradation of mutant protein, or their combinations. During the course of examining the primary cause for deficient enzyme activity, Ishii *et al.* [30,31] examined the kinetic properties and stabilities of several mutant enzymes found in cardiac variants. Following the same approach, we recently studied various disease-causing mutations that have been identified in patients who present with residual enzyme activity regardless of clinical phenotype [32]. Sixteen mutant enzymes, including ten mutations identified in variant patients (A20P, E66Q, M72V, I91T, R112H, F113L, N215S, Q279E, M296I, and M296V), four mutations found in classic patients (E59K, A156V, L166V, and R356W), and two mutations present in both variant and classic patients (A97V and R301Q) were efficiently purified from transfected COS-7 cells, and their enzymatic and biochemical properties examined. The cardiac mutations typically present relatively higher residual enzyme activity compared to the classic mutations. Except for one mutation (E59K), all mutant proteins appeared to have normal K_m and V_{max} values, indicating that they retain full or partial catalytic activity. The K_m and V_{max} values for the E59K mutant deviated largely from those of the wild-type enzyme, indicating that this mutation causes impaired kinetic activity. Although all of the mutant enzymes examined showed the same optimal pH as the wild-type enzyme, the mutant enzymes were substantially less stable compared to the wild-type enzyme. Western blot analysis of mutant enzymes expressed in transfected COS-7 cells and patient fibroblasts demonstrated that most mutant enzymes had low protein yields, indicating that excessive degradation of the mutant enzyme could be directly responsible for deficient enzyme activity caused by these missense mutations.

In studies of intracellular trafficking and processing of mutant α-Gal A enzymes, the R301Q and L166V mutant enzymes were not processed even after 24 h, as determined by a metabolic labeling and pulse-chase study [32]. The degradation of mutant protein was observed at 6 h after they were synthesized. Subcellular fractionation indicated that neither enzyme activity, nor mutant protein could be detected in the lysosomal fractions of transfected COS-7 cells. Only a small